NEW CONSTRAINTS FROM CRISM AND MASTCAM SPECTRA ON THE MINERALOGY AND ORIGIN OF MT. SHARP GEOLOGIC UNITS, GALE CRATER, MARS. B. Horgan[1], A. A. Fraeman[2], M. S. Rice[3], J. F. Bell III[4], D. Wellington[4], J. J. Johnson[5]. [1]Purdue University (briony@purdue.edu), [2]Jet Propulsion Laboratory, [3]Western Washington University, [4]Arizona State University, [5]Johns Hopkins/Applied Physics Lab.

Introduction: Mars Science Laboratory (MSL) is currently exploring the lowermost units of Mt. Sharp inside of Gale Crater. To date, the mineralogy of Mt. Sharp has been based on analysis of orbital spectra from the CRISM imaging spectrometer [1-4]. In this study, we seek to use Mastcam visible spectra (445-1013 nm) along with CRISM VNIR spectra (typically 400-2600 nm) in order to better constrain the mineralogy and origin of the mound units, to aid in planning the future traverse of MSL, and to help place MSL results in their broader straigraphic context. Mastcam is a pair of cameras [5] with 3 broadband Bayer RGB and 8 narrowband filters that have the potential to contribute new information on the mineralogy of the mound. Key absorption bands for Fe-bearing phases are located at these wavelengths, where CRISM spectra have reduced sensitivity. Mastcam images also have superior spatial resolution, allowing for more detailed correlation of units with morphologic features. By applying new analysis techniques to Mastcam images, here we report the identification of refined mineralogical units within Mt. Sharp.

CRISM Observations: CRISM analyses (Figure 1) have identified a strong ~900 nm absorption band, most consistent with hematite, associated with both the Murray formation that comprises the lowermost units of Mt. Sharp, as well as a resistant ridge unit at higher elevations [1-3]. Hematite has been confirmed in the Murray during *in situ* invesgitgations by MSL [e.g., 6]. Noncontiguous segments of the hematite ridge extend around the mound to the SW corner at variable elevations [4]. In the NW where MSL will traverse, a trough immediately behind the ridge exhibits Fe/Mg-smectite absorption bands near 2300 nm [1]. Along the W side of the mound, hematite appears at a similar stratigraphic level as smectites [4]. Consistently above the smectites, a distinct bench-forming unit exhibits strong red spectral slopes between 1-1.8 μm that is consistent with ferrous iron, either in olivine [1] or in ferrous iron-bearing alteration phases [4,7]. Various sulfates are also detected throughout the mound, and are the main spectral signature detected in the units above the ridge [1,4].

Mastcam Analysis: Mastcam images of the mound from sol 468 and 1104 were analyzed for this study (Fig. 3). In order to produce spectral maps from Mastcam images, first the scenes were masked to remove shadows (dark at long wavelengths), sky, and specular reflection (both bright at short wavelengths). Next, the spectral parameters in Table 1 are calculated for the scene, and are used to define and map the distribution of the spectral units in Table 2. These six distinct spectral units generally correspond spatially to units prevsiouly identified by CRISM.

New spectral units within the hematite ridge: CRISM and Mastcam both detect the ~880 nm band due to hematite in the ridge, which is supported by Chemcam observations [2,8,9]; however, Mastcam mapping indicates that the ridge also contains a second major spectral unit. This unit also exhibits a broad abosorption near ~900 nm, but with a band center shifted closer to 950 nm (Fig 2). This unit also has a weaker red spectral slope at long wavelengths than the hematite, but looks similar to hematite at short wavelengths. This spectral shift is too large to be explained by variations in hematite grain size [10], so this suggests another phase must be present. Both goethite and nontronite exhibit bands centered near 920-950 nm and appear similar to hematite at shorter wavelengths. In addition, a mixture with another mafic mineral, e.g., pyroxene, could cause this shift – however, as the ridge does not exhibit pyroxene or phyllosilicate bands in CRISM VNIR spectra [2,4], goethite is more likely.

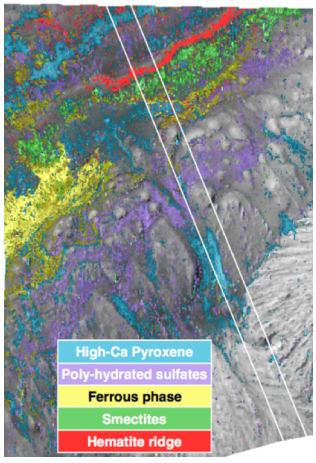

Figure 1: *Unit map for CRISM image FRTB6F1 [4]. White lines are limits of view for Fig. 3.*

Table 1: *Mastcam spectral parameters*

Parameter	Definition	Rationale	Bands
BD527R	Band depth at 527nm, shoulders at 445/805	Detects ~550nm band due to ferric phases	R123
BD800R	Band depth at 805nm, shoulders at 527/1013	Detects flattening due to ferrous phases	R136
BD905R	Band depth at 908nm, shoulders at 805/1013	Detects ~900nm band due to ferric phases	R346
BD935R	Band depth at 937nm, shoulders at 805/1013	Detects various Fe-absorption bands	R356
SH1012R	Reflectance ratio, 908 nm / 1012 nm	Postive in Fe-clays, negative in mafics	R35
MAXR	Channel with maximum reflectance	High for hematite, low for ferrous	R3456

Table 2: *Mastcam spectral units*

Interp.	MAXR	BD527R	BD800R	Other
Pyroxene	< 900 nm		< -0.3	SH1012R < 0.95 BD935R > 0.02
Olivine	< 900 nm	< 0.05	> -0.3	
Hematite	> 950 nm	> 0.05		BD905R > 0.02
Goethite	< 950 nm	> 0.05	> -0.3	
Dust	< 950 nm	< 0.05	< -0.3	R(800nm) > 0.25

Possible ferrous alteration phases in the mound: The ferrous unit in the mound exhibits CRISM VNIR spectra that are consistent with both olivine and ferrous alteration phases. However, where this unit is exposed in outcrop along the edge of the fan and as light toned mounds above the hematite ridge, it exhibits a characteristic flattening in Mastcam spectra between 650-800 nm that occasionally deepens to form an absorption band near 750 nm (purple in Fig 2) [8]. While this spectral shape does not appear to be consistent with olivine (note that a distinct olivine spectral shape is detected in the dunes), it may be consistent with ferrous phyllosilicates like celadonite, chlorite, or ferrous smectites.

Primary mineralogy of mound sediments: Dark-toned sediments on the mound exhibit CRISM spectra consistent with high-Ca pyroxene [4], which is distinct from the olivine signatures exhibited by the Bagnold dunes and confirmed *in situ* by MSL [11]. Mastcam spectra shown in Fig 2 can detect the spectral difference between the dunes (navy) and the mound sediments (blue), although the spectral signature of both is non-unique to olivine vs. pyroxene at Mastcam wavelengths.

Implications: The presence of goethite within the hematite ridge could be due to variable redox conditions during deposition of ridge sediments, which could represent a key energy source for microbes. Indeed, if reduced iron alteration phases are present in the ferrous unit as well, this could support the presence of a redox gradient within the mound. This relationship is consistent with previous hypotheses for the origin of the ridge, where reduced Fe-bearing fluids emerged into an oxidizing environment [2]. MSL will test this hypothesis *in situ* after arriving at the hematite ridge in 2017.

In addition, Mastcam observations of pyroxene in sediments mantling Mt. Sharp may suggest that Mt. Sharp is a significant souce of sediments, and that the distinct spectral difference compared to the olivine-rich dunes will allow MSL to test this hypothesis as we move toward the mound. This hypothesis would also constrain the origin of the upper mound units – the presence of significant sand-sized pyroxene in the upper mound is inconsistent with airfall dust, and instead suggests a fluvial, aeolian, or pyroclastic origin. This study demonstrates that multispectral imaging with Mastcam is a significant supplement to orbital VNIR mapping and will be key for guiding MSL investigations in the future.

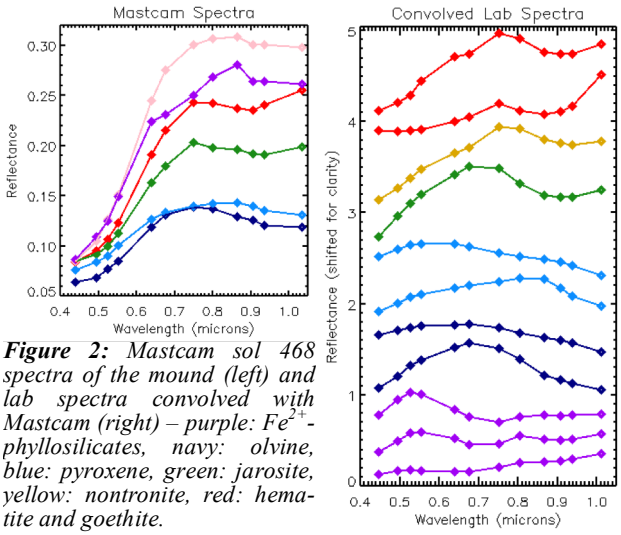

Figure 2: *Mastcam sol 468 spectra of the mound (left) and lab spectra convolved with Mastcam (right) – purple: Fe^{2+}-phyllosilicates, navy: olivine, blue: pyroxene, green: jarosite, yellow: nontronite, red: hematite and goethite.*

References: [1] Milliken *et al*. (2010) *GRL 37*, doi:10.1029/2009GL041870. [2] Fraeman *et al*. (2013) *Geology 41*, 1103-1106. [3] Fraeman *et al.* (2016) *JGR, accepted.* [4] Rice *et al.* (2015) *AGUFM,* #P43D-2144. [5] Kinch et al. (2013) LPSC 44, #1061. [6] Cavanagh *et al*. (2015) *LPSC*, #2735. [7] Horgan (2015) *AbSciCon,* #7463. [8] Johnson et al (2016) *Am. Min. 101*, 1501-1514. [9] Wellington et al (2016) *Am. Min.,* accepted. [10] Morris *et al*. (1985) *JGR 90*, 3126-3144. [11] Achilles *et al*. (2016) *LPSC*, #2532.

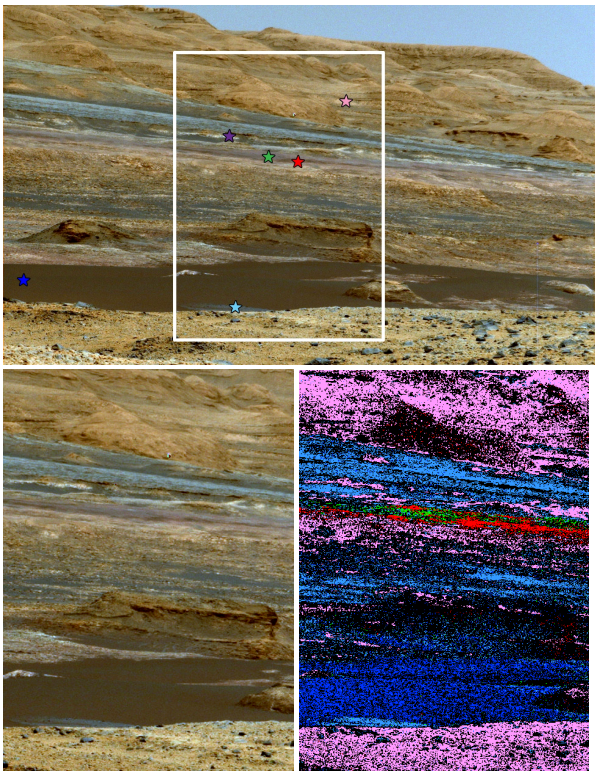

Figure 3: *(top) Mastcam image in false color from sol 468, stars are locations of Fig 2 spectra. (bottom) Zoom compared to spectral unit map, colors correspond to Fig 2 spectra.*